NANO LETTERS

Letter

pubs.acs.org/NanoLett

Stretching-Induced Conductance Increase in a Spin-Crossover Molecule

Riccardo Frisenda,[†] Gero D. Harzmann,[‡] Jose A. Celis Gil,[†] Joseph M. Thijssen,[†] Marcel Mayor,*[,‡,¶,§] and Herre S. J. van der Zant*[,†]

[†]Kavli Institute of Nanoscience, Delft University of Technology, 2600 GA Delft, The Netherlands

[‡]University of Basel, 4056 Basel, Switzerland

[¶]Karlsruhe Institute of Technology (KIT), P.O. Box 3640, 76021 Karlsruhe, Germany

[§]Lehn Institute of Functional Materials (LIFM), Sun Yat-Sen University (SYSU), Gunagzhou, China

Supporting Information

ABSTRACT: We investigate transport through mechanically triggered single-molecule switches that are based on the coordination sphere-dependent spin state of Fe^{II}-species. In these molecules, in certain junction configurations the relative arrangement of two terpyridine ligands within homoleptic Fe^{II}-complexes can be mechanically controlled. Mechanical pulling may thus distort the Fe^{II} coordination sphere and eventually modify their spin state. Using the movable nanoelectrodes in a mechanically controlled break-junction at low temperature, current−voltage measurements at cryogenic temperatures support the hypothesized switching mechanism based on the spin-crossover behavior. A large fraction of molecular junctions formed with the spin-crossover-active Fe^{II}-complex displays a conductance increase for increasing electrode separation and this increase can reach 1−2 orders of magnitude. Theoretical calculations predict a stretching-induced spin transition in the Fe^{II}-complex and a larger transmission for the high-spin configuration.

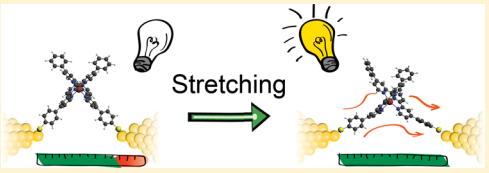

KEYWORDS: *Spin-crossover switch, nanoscale transport, molecular spintronics, density functional theory*

Control over the molecular conductance by means of an external stimulus is an interesting concept in molecular scale electronics and different single-molecule switches are known in literature.[1−4] In the most common design, the molecule contains chemical groups that can switch between two or more stable configurations, like dithienylethene or azobenzene groups.[5−9] Depending on the system, the conductance can be tuned by means of light,[10,11] mechanical manipulation,[12−15] electrochemical gating,[16,17] the applied bias voltage[18] or by the current.[6,19]

The spin-crossover (SCO) phenomenon[20−22] can lead to bistability, as was observed recently in some metal-containing molecules and compounds.[23−25] A spin-crossover molecule exhibits two different ground states, each of them stable under certain conditions and characterized by different values of the molecular spin. Among the various metal atoms, the complexes of iron(II) are the most investigated ones.[26] When the iron atom is surrounded by an octahedral ligand environment (ligand field), its five spin-degenerate 3d levels split into a doublet and a triplet, as shown in Figure 1b. The filling order of these levels with the six electrons of Fe^{II} depends on the ratio between the ligand field energy, E_{LF}, and the spin exchange energy, E_{EXC}. If $E_{LF} \gg E_{EXC}$, the electrons are all paired up and the triplet is completely filled, giving a total spin $S = 0$. In the opposite case, $E_{EXC} \gg E_{LF}$, the levels are filled according to Hund's rule and the spin is maximized reaching a value $S = 2$. The first case is defined as the low-spin (LS) state and the second one as the high-spin (HS) state. Different stimuli, like pressure or temperature, have been used to vary the ratio E_{EXC}/E_{LF} to control the SCO state. Apart from the total spin, the LS and HS states present differences in geometry, electronic structure, and highest occupied molecular orbital−lowest unoccupied molecular orbital (HOMO−LUMO) gap energy. According to theoretical predictions[27] and low-temperature scanning tunnel microscopy (STM) experiments,[23,24] the HS state is more conducting than the LS state.

In our study, we propose to modify the spin state of Fe^{II} terpyridine complexes mechanically. The concept and the molecular design are displayed in Figure 1. The SCO active center is the Fe^{II} complex **1**, consisting of two terpyridine (tpy) ligands that are further phenyl functionalized in 4 and 4″ positions. For each ligand, one of both phenyl rings is decorated with a thiol group in the para position as anchor group that is known to have considerable mechanical stability on gold electrodes.[28−30] In certain junction arrangements, the geometry of the coordination sphere provided by the two terpyridine ligands should depend on the electrodes spacing and thus become tunable by mechanical manipulation.

The intended SCO-based switching mechanism is sketched in Figure 1a−c. When the tpy ligands are arranged

Received: December 1, 2015
Revised: April 14, 2016
Published: April 18, 2016

DOI: 10.1021/acs.nanolett.5b04899
Nano Lett. 2016, 16, 4733−4737

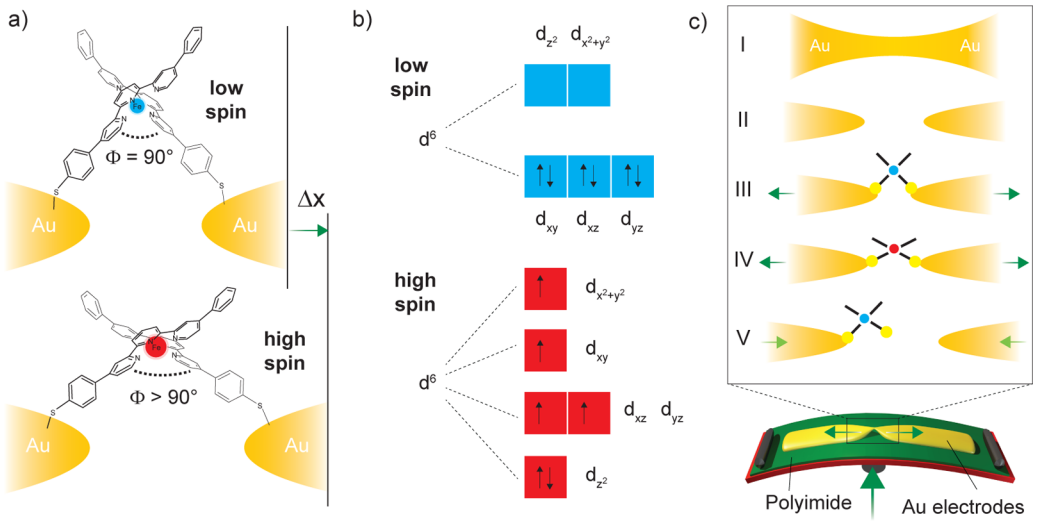

Figure 1. Two-terminal mechanically controlled single-molecule junction. (a) Sketch of the Fe^{II}-based SCO molecular junction in the ideal arrangement to trigger the LS to HS switch by separating the electrodes by Δx. (b) $Iron^{II}$ 3d levels involved in the spin-crossover phenomenon. (c) Schematic illustration of a MCBJ setup (bottom) with the molecule placed in the junction as sketched in (a). A freely suspended gold bridge, built on a flexible substrate, is elongated upon bending the substrate in a mechanically controlled three-point bending mechanism. The predefined breaking point of the gold structure is enlarged on the top of the figure at different stages of the experiment: (I) elongation of the gold wire with the help of the pushing rod and two opposing counter supports (see bottom of the figure). (II) Rupture of the gold wire resulting in the formation of two gold nanoelectrodes facing each other. (III) The metal complex may bridge both nanoelectrodes and (IV) eventually one could manipulate the spatial arrangement of the complexe's ligands by stretching of the junction. After the final rupture of the junction, the electrodes can be moved toward each other (V) to start a new experiment.

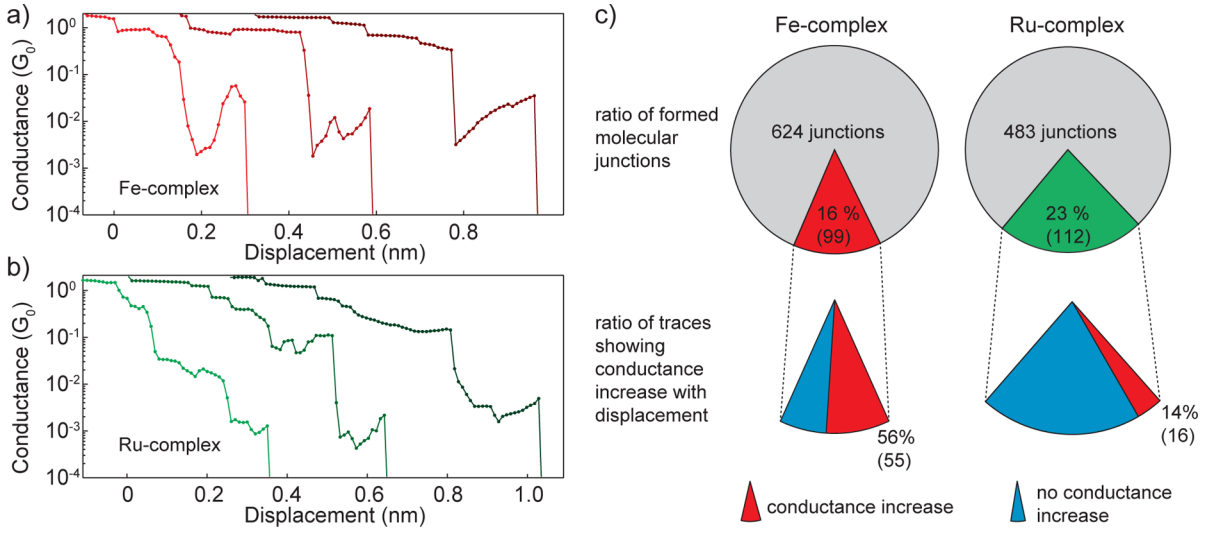

Figure 2. Conductance measurements. (a,b) Three examples of conductance traces as a function of electrode displacement measured respectively in the presence of the Fe^{II}-complex and Ru^{II}-complex. (c) Junction-formation statistics and percentage of molecular junctions showing a conductance increase.

perpendicularly, the complex is in the LS state. Upon increasing the electrode separation, the ligands are pulled further apart and the distortion of the perpendicular arrangement of the two tpy ligands leads to a reduction of E_{LF}. For large enough distortion, the exchange energy will dominate over the ligand field energy thereby triggering the switch from the LS to the HS state. With both ligands bearing the thiol anchor group in the para position with respect to the coordinating pyridine nitrogen, the coordinated central ion is part of the current path, and alterations in its spin state are expected to be reflected in the junctions transport characteristics.[23,24,31] In order to trace the SCO nature of the phenomenon, we also investigate the corresponding Ru^{II} complex **2**, which due to the considerable larger crystal field strength is expected not to be subjected to mechanically triggered spin alterations.

For the synthesis of the tpy ligand and the corresponding complexes **1** and **2**, we mainly adapted already reported procedures[25,32] and the corresponding protocols are provided in the Supporting Information together with the analytical data. To contact the molecule **1** or **2**, we use a mechanically controlled break junction (MCBJ) providing two gold nanoelectrodes of adjustable distance. Figure 1c shows a schematics of the MCBJ setup together with a sketch of the molecular junction formation.

Briefly, an MCBJ sample consists of a gold wire deposited on top of a flexible substrate (I). Bending the substrate results in

DOI: 10.1021/acs.nanolett.5b04899
Nano Lett. 2016, 16, 4733−4737

the thinning of the wire until its rupture, which leaves two sharp gold extremities facing each other (II). The two tips can be used as nanoelectrodes and eventually a molecule can bridge the gap (III); for specific junction arrangements, the geometry of the complexes can be changed by separating the electrodes (IV) until the rupture of the molecular junction. During the stretching of the wire, we measure current−voltage (I−V) characteristics at each position in steps of 0.02 nm, until the noise level of the setup is reached ($I \sim 20$ pA). By pushing the electrodes together we reform the wire (V) and a new breaking experiment can start by repeating the above procedure. All the measurements were performed in high vacuum ($p \sim 10^{-7}$ mbar) and cryogenic temperature ($T \sim 6$ K). Before each experiment, we deposit the target molecule on the MCBJ sample by fully immersing for 4 h the sample in a vial containing a 1 mmol/L solution of the protected thiol-bearing species. After that time, we remove the sample from the solution, rinse it with pure solvent (acetonitrile), and mount it in the MCBJ setup. The setup is evacuated and then cooled in a liquid helium bath.

After the rupture of the gold wire in the presence of molecule **1** in 84% of the traces (525 out of 624), the conductance decays exponentially as a function of displacement. This behavior, typical of vacuum tunneling, indicates that no molecule bridges the electrodes. In the remaining 16% of the traces (99 traces; a typical yield for these measurements), the presence of plateaus and steps and the absence of an exponential and monotonous decrease in the conductance versus distance indicate that a molecule is bridging the electrodes. Plots of the conductance versus electrode displacement often show an increase in the molecular conductance during the stretching in case of junctions formed with molecule **1**; a few examples are shown in Figure 2a. Among the 99 molecular junctions, 55 traces show a conductance increase while stretching, corresponding to 56% of the molecular junctions. The increase can be more than 1 order of magnitude; see Section 7 of the Supporting Information for the collective plots of the conductance traces falling in each category and for a comparison.

Junctions formed with the reference molecule **2**, where the central Fe^{II} ion is substituted by a Ru^{II} ion, show substantially less frequently an increase in the conductance versus electrode-displacement traces and the increase is less pronounced. In 111 molecular junctions formed, only in 16 traces an increase in conductance during the stretching is present, corresponding to 14% of the molecular junctions. Typical conductance-displacement traces are shown in Figure 2b. Figure 2c displays the statistics for molecules **1** and **2**. The statistics indicates that the observation of an increase in conductance versus stretching is both more frequent and more pronounced in the junctions formed with the Fe-complex with respect to the ones with the Ru-complex.

To quantify the conductance increase, we extract from each conductance trace the ratio between the low-conductance value, where the conductance starts to increase, and the highest conductance reached after stretching. Figure 3a presents histograms of the high/low conductance ratio extracted for all 55 and 16 junctions exhibiting a conductance increase, formed with molecules **1** and **2** respectively. The x-axis is binned logarithmically. For molecule **1**, the skewed distribution presents a tail that reaches values near 70, whereas for molecule **2** the distribution vanishes beyond 7. From the histograms, it is evident that the molecular junctions formed with Fe-complexes show on average a larger increase in conductance versus stretching than the Ru-complex junctions. In order to make the differences between the Fe^{II} and Ru^{II} molecules clearer, we subtracted the normalized histogram recorded for the Ru^{II} junctions from the histogram obtained for the Fe^{II} junctions (see Section 10 of the Supporting Information for details about the histograms subtraction). The resulting histogram in Figure 3b clearly shows the larger number of counts in the case of Fe^{II} at large values of increase in conductance.

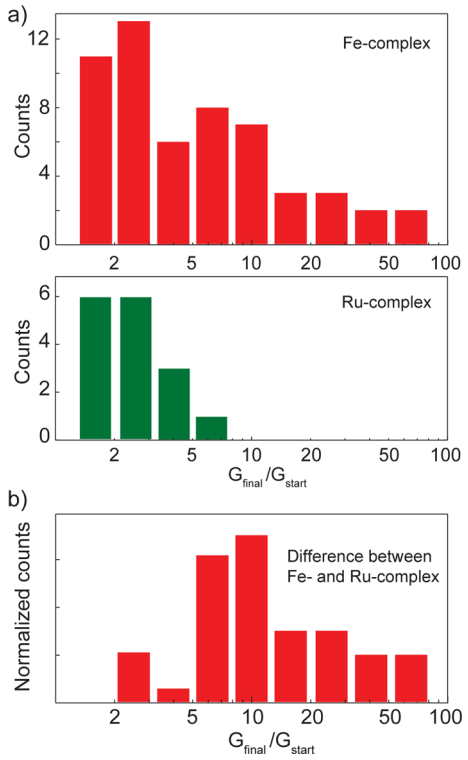

Figure 3. Statistics of conductance increase. (a) Histogram of the values of increase in conductance for molecular junctions containing Fe (top) and Ru (bottom) complexes. The x-axis is binned logarithmically. (b) Difference between the conductance ratio histograms of Fe^{II} and Ru^{II} after normalization (see Supporting Information).

Finally, we study the transition from the LS state to the HS state theoretically using density functional theory (DFT) calculations. For both states individually, we perform a geometrical relaxation of the Fe^{II} complex **1** in gas phase. Then we stretch or compress the molecule by changing the distance between the sulfur atoms, perform a geometric relaxation, and calculate the energies. For this calculation, we use the ADF quantum chemistry package with a TZP-basis of atomic orbitals and the B3LYP functional. In Figure 4a, we plot the energy for the low-spin and high-spin states as a function of the separation between the sulfur atoms. We define the separation of 16.03 Å as the zero, corresponding to an angle of 90° between the two tpy-subunits. For short stretching distances up to 3 Å, the LS state is more favorable. At a stretching of 3.5 Å, a crossover to a regime where the HS state is the stable one occurs. The relaxed molecular geometries for both states are shown in Figure 4b for a sulfur−sulfur separation, respectively, of 16.03 Å (LS) and 20.52 Å (HS). The angle between the two tpy central units is equal to 90° and 101°, respectively.

DOI: 10.1021/acs.nanolett.5b04899
Nano Lett. 2016, 16, 4733−4737

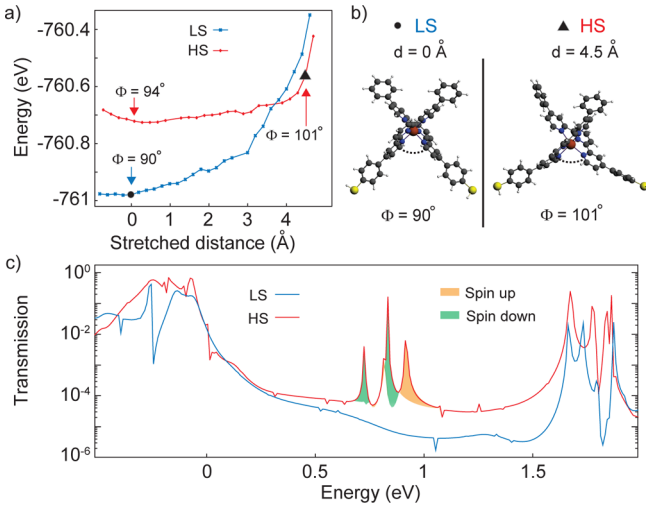

Figure 4. Theoretical calculations. (a) Energy of the LS and HS states as a function of stretching distance found from DFT calculations. (b) Relaxed geometries of the LS and HS states at the stretching distance of 0 and 4.5 Å respectively. (c) Total transmission of the LS and HS geometries shown in (b) in a metal−molecule−metal configuration calculated with self-consistent DFT-NEGF. The shaded areas correspond to spin polarized transmission for up (orange) or down (green) spin electrons. The Fermi energy of the contacts is at 0 eV.

To analyze the transport properties of the two states, we perform self-consistent DFT-NEGF calculations for the molecules attached to a face-centered cubic (111) gold surface. For our calculations, we use a TZP-basis of numerical atomic orbitals on the molecule, a SZ-basis of numerical atomic orbitals on the gold atoms and the GGA PBE functional in our implementation of the NEGF-based transport in the ADF/band quantum chemistry package. Figure 4c compares the mean transmissions for the LS and HS states as a function of the energy, with the Fermi energy at 0 eV. In the region of the HOMO−LUMO gap, between 0 and 1.5 eV, the HS state shows a larger transmission than the LS state. We further notice that the HS state transmission shows a certain degree of spin-polarization, evidenced in Figure 4b, while the LS transmission is not spin-polarized (see also Section 9 in the Supporting Information). Thus, the calculations predict for the Fe^{II} complex **1** the presence of a stretching-induced SCO transition that is accompanied by an increase in conductance when going from the LS to the HS state.

Apart from the HS−LS transition, predicted in the case of the Fe^{II} complex **1**, other mechanisms can increase the conductance of a molecular junction while stretching the electrodes.[33,34] Bruot et al.[15] found that even simple molecules like benzene dithiol immobilized in molecular junctions formed with gold electrodes at low temperature can show a conductance increase while stretching. This conductance modulation is attributed to a stretching-induced better alignement of the HOMO with the Fermi energy of the electrodes. If this more favorable level alignment compensates the decrease in electronic coupling, the conductance will increase for larger displacement. Although we cannot exclude that this mechanism may also play a role here, we expect that the level shifts are smaller in our more extended molecules.

Alternatively, in the molecules studied here, the tpy ligands may also be important for charge transport from one electrode to the other. Specifically, the angle Φ between the two flat tpy groups (indicated in Figure 1a) can influence the transport through the molecule.[35,36] Considering the overlap of the two tpy π-systems, in a first approximation the closer the angle is to 90° the smaller the conductance of the molecule,[37] independently from the central metal atom species. Figure S29 of the Supporting Information shows the transmission calculated for the Fe^{II} complex in a stretched configuration (stretching distance of 4.5 Å, see Figure 4a). These calculations indicate that the transmission of the low-spin complex increases as the molecule is stretched. Thus, this mechanism can occur for both Fe and Ru molecules, irrespective of the SCO transition, with the central metal ion acting exclusively as a mechanical joint between both tpy ligands[38] and not as a charge transport channel. The increased coupling bertween the two terpy groups can explain the increase in conductance observed in some of the junctions formed with the Ru^{II} complex, where an SCO is not expected.

In summary, we have studied transport through mechanically switchable Fe^{II} spin crossover molecules. Using mechanically controllable gold nanoelectrodes, we monitor the zero-bias conductance while stretching the electrodes. In more than half of the molecular junctions, an increase in conductance that can reach 2 orders of magnitude has been observed. To understand the origin of this conductance feature, we investigated a reference compound that contains a Ru^{II} ion for which a SCO transition is not expected to occur. In the Ru^{II}, an increase in conductance versus stretching is also observed but substantially less frequently, and when it occurs the increase is on average smaller than for the Fe^{II} case. The comparison between the two metal centers suggests that small conductance increases can be induced by stretching these molecules independently from the central atom type but that the inclusion of the SCO-active Fe^{II} ion gives larger and more frequent conductance increases. Theoretical calculations indicate that the SCO transition can be triggered by pulling on the terminal sulfur atoms of the Fe^{II} complex and that the high-spin state, energetically more favorable in the stretched molecule, has a larger zero-bias conductance than the low-spin state.

■ ASSOCIATED CONTENT

Supporting Information

The Supporting Information is available free of charge on the ACS Publications website at DOI: 10.1021/acs.nanolett.5b04899.

Molecular synthesis and characterization of the data compounds. Additional data of the single-molecule experiments. Additional details about DFT calculations. (PDF)

■ AUTHOR INFORMATION

Corresponding Authors

*E-mail: marcel.mayor@unibas.ch.
*E-mail: h.s.j.vanderzant@tudelft.nl.

Author Contributions

R.F. and G.D.H. contributed equally to the work.

Notes

The authors declare no competing financial interest.

■ ACKNOWLEDGMENTS

We acknowledge financial support by the European FP7-ITN network MOLESCO, the Swiss National Science Foundation (Grant 200020-159730), the Dutch funding agencies NWO/

DOI: 10.1021/acs.nanolett.5b04899
Nano Lett. 2016, 16, 4733−4737

OCW and the Dutch organization for Fundamental Research (FOM), and an ERC advanced grant (Mols@Mols).

REFERENCES

(1) Feringa, B. L. *Molecular switches*; Wiley: New York, 2001.
(2) Weibel, N.; Grunder, S.; Mayor, M. *Org. Biomol. Chem.* **2007**, *5*, 2343.
(3) van der Molen, S. J.; Liljeroth, P. *J. Phys.: Condens. Matter* **2010**, *22*, 133001.
(4) Sun, L.; Diaz-Fernandez, Y. A.; Gschneidtner, T. A.; Westerlund, F.; Lara-Avila, S.; Moth-Poulsen, K. *Chem. Soc. Rev.* **2014**, *43*, 7378.
(5) Irie, M. *Chem. Rev.* **2000**, *100*, 1685.
(6) Choi, B. Y.; Kahng, S. J.; Kim, S.; Kim, H.; Kim, H. W.; Song, Y. J.; Ihm, J.; Kuk, Y. *Phys. Rev. Lett.* **2006**, *96*, 156106.
(7) Henningsen, N.; Franke, K. J.; Torrente, I. F.; Sehulze, G.; Priewisch, B.; Ruck-Braun, K.; Dokic, J.; Klamroth, T.; Saalfrank, P.; Pascual, J. I. *J. Phys. Chem. C* **2007**, *111*, 14843.
(8) Tam, E. S.; Parks, J. J.; Shum, W. W.; Zhong, Y. W.; Santiago-Berrios, M. B.; Zheng, X.; Yang, W.; Chan, G. K.; Abruna, H. D.; Ralph, D. C. *ACS Nano* **2011**, *5*, 5115.
(9) Kim, Y.; Hellmuth, T. J.; Sysoiev, D.; Pauly, F.; Pietsch, T.; Wolf, J.; Erbe, A.; Huhn, T.; Groth, U.; Steiner, U. E.; Scheer, E. *Nano Lett.* **2012**, *12*, 3736.
(10) Hwang, J.; Pototschnig, M.; Lettow, R.; Zumofen, G.; Renn, A.; Gotzinger, S.; Sandoghdar, V. *Nature* **2009**, *460*, 76.
(11) Lara-Avila, S.; Danilov, A. V.; Kubatkin, S. E.; Broman, S. L.; Parker, C. R.; Nielsen, M. B. *J. Phys. Chem. C* **2011**, *115*, 18372.
(12) Quek, S. Y.; Kamenetska, M.; Steigerwald, M. L.; Choi, H. J.; Louie, S. G.; Hybertsen, M. S.; Neaton, J. B.; Venkataraman, L. *Nat. Nanotechnol.* **2009**, *4*, 230.
(13) Kim, Y.; Song, H.; Strigl, F.; Pernau, H. F.; Lee, T.; Scheer, E. *Phys. Rev. Lett.* **2011**, *106*, 196804.
(14) Meisner, J. S.; Kamenetska, M.; Krikorian, M.; Steigerwald, M. L.; Venkataraman, L.; Nuckolls, C. *Nano Lett.* **2011**, *11*, 1575.
(15) Bruot, C.; Hihath, J.; Tao, N. *Nat. Nanotechnol.* **2011**, *7*, 35−40.
(16) Darwish, N.; Diez-Perez, I.; Guo, S. Y.; Tao, N. J.; Gooding, J. J.; Paddon-Row, M. N. *J. Phys. Chem. C* **2012**, *116*, 21093.
(17) Baghernejad, M.; Zhao, X. T.; Ornso, K. B.; Fueg, M.; Moreno-Garcia, P.; Rudnev, A. V.; Kaliginedi, V.; Vesztergom, S.; Huang, C. C.; Hong, W. J.; Broekmann, P.; Wandlowski, T.; Thygesen, K. S.; Bryce, M. R. *J. Am. Chem. Soc.* **2014**, *136*, 17922.
(18) Qiu, X. H.; Nazin, G. V.; Ho, W. *Phys. Rev. Lett.* **2004**, *93*, 196806.
(19) Liljeroth, P.; Repp, J.; Meyer, G. *Science* **2007**, *317*, 1203.
(20) Cambi, L.; Szego, L. *Ber. Dtsch. Chem. Ges. B* **1931**, *64*, 2591.
(21) Gutlich, P. *Eur. J. Inorg. Chem.* **2013**, *2013*, 581.
(22) Ruiz, E. *Phys. Chem. Chem. Phys.* **2014**, *16*, 14.
(23) Miyamachi, T.; Gruber, M.; Davesne, V.; Bowen, M.; Boukari, S.; Joly, L.; Scheurer, F.; Rogez, G.; Yamada, T. K.; Ohresser, P.; Beaurepaire, E.; Wulfhekel, W. *Nat. Commun.* **2012**, *3*, 938.
(24) Gopakumar, T. G.; Matino, F.; Naggert, H.; Bannwarth, A.; Tuczek, F.; Berndt, R. *Angew. Chem., Int. Ed.* **2012**, *51*, 6262.
(25) Harzmann, G. D.; Frisenda, R.; van der Zant, H. S. J.; Mayor, M. *Angew. Chem., Int. Ed.* **2015**, *54*, 13425−13430.
(26) Gutlich, P.; Gaspar, A. B.; Garcia, Y. *Beilstein J. Org. Chem.* **2013**, *9*, 342.
(27) Aravena, D.; Ruiz, E. *J. Am. Chem. Soc.* **2012**, *134*, 777.
(28) Hakkinen, H. *Nat. Chem.* **2012**, *4*, 443.
(29) Haiss, W.; Wang, C.; Grace, I.; Batsanov, A. S.; Schiffrin, D. J.; Higgins, S. J.; Bryce, M. R.; Lambert, C. J.; Nichols, R. J. *Nat. Mater.* **2006**, *5*, 995.
(30) Frisenda, R.; Tarkuc, S.; Galan, E.; Perrin, M. L.; Eelkema, R.; Grozema, F. C.; van der Zant, H. S. J. *Beilstein J. Nanotechnol.* **2015**, *6*, 1558−1567.
(31) Gruber, M.; Davesne, V.; Bowen, M.; Boukari, S.; Beaurepaire, E.; Wulfhekel, W.; Miyamachi, T. *Phys. Rev. B: Condens. Matter Mater. Phys.* **2014**, *89*, 195415.
(32) Harzmann, G. D.; Neuburger, M.; Mayor, M. *Eur. J. Inorg. Chem.* **2013**, *2013*, 3334.
(33) Andrews, D. Q.; Cohen, R.; Van Duyne, R. P.; Ratner, M. A. *J. Chem. Phys.* **2006**, *125*, 174718.
(34) Kamenetska, M.; Koentopp, M.; Whalley, A. C.; Park, Y. S.; Steigerwald, M. L.; Nuckolls, C.; Hybertsen, M. S.; Venkataraman, L. *Phys. Rev. Lett.* **2009**, *102*, 126803.
(35) Solomon, G. C.; Andrews, D. Q.; Van Duyne, R. P.; Ratner, M. A. *ChemPhysChem* **2009**, *10*, 257.
(36) Venkataraman, L.; Klare, J. E.; Nuckolls, C.; Hybertsen, M. S.; Steigerwald, M. L. *Nature* **2006**, *442*, 904.
(37) Woitellier, S.; Launay, J. P.; Joachim, C. *Chem. Phys.* **1989**, *131*, 481.
(38) Ruben, M.; Landa, A.; Lortscher, E.; Riel, H.; Mayor, M.; Gorls, H.; Weber, H. B.; Arnold, A.; Evers, F. *Small* **2008**, *4*, 2229.

DOI: 10.1021/acs.nanolett.5b04899
Nano Lett. 2016, 16, 4733−4737